Theoretical and Applied Climatology
https://doi.org/10.1007/s00704-018-2474-9

ORIGINAL PAPER

Assessment of the impact of climate change on spatiotemporal variability of blue and green water resources under CMIP3 and CMIP5 models in a highly mountainous watershed

Iman Fazeli Farsani[1] · **M. R. Farzaneh**[2] · **A. A. Besalatpour**[3] · **M. H. Salehi**[1] · **M. Faramarzi**[4]

Received: 5 December 2016 / Accepted: 2 April 2018

Abstract

The variability and uncertainty of water resources associated with climate change are critical issues in arid and semi-arid regions. In this study, we used the soil and water assessment tool (SWAT) to evaluate the impact of climate change on the spatial and temporal variability of water resources in the Bazoft watershed, Iran. The analysis was based on changes of blue water flow, green water flow, and green water storage for a future period (2010–2099) compared to a historical period (1992–2008). The r-factor, p-factor, R^2, and Nash–Sutcliff coefficients for discharge were 1.02, 0.89, 0.80, and 0.80 for the calibration period and 1.03, 0.76, 0.57, and 0.59 for the validation period, respectively. General circulation models (GCMs) under 18 emission scenarios from the IPCC's Fourth (AR4) and Fifth (AR5) Assessment Reports were fed into the SWAT model. At the sub-basin level, blue water tended to decrease, while green water flow tended to increase in the future scenario, and green water storage was predicted to continue its historical trend into the future. At the monthly time scale, the 95% prediction uncertainty bands (95PPUs) of blue and green water flows varied widely in the watershed. A large number (18) of climate change scenarios fell within the estimated uncertainty band of the historical period. The large differences among scenarios indicated high levels of uncertainty in the watershed. Our results reveal that the spatial patterns of water resource components and their uncertainties in the context of climate change are notably different between IPCC AR4 and AR5 in the Bazoft watershed. This study provides a strong basis for water supply-demand analyses, and the general analytical framework can be applied to other study areas with similar challenges.

Keywords Water resource management · RCP emission scenarios · Prediction uncertainty · SWAT model

1 Introduction

Changes in the hydrological cycle due to climate change can affect water resource availability (IPCC 2014), and their impact can differ among regions. Irregular distribution of precipitation patterns and high temperatures are major concerns for the access, availability, and uses of water resources (Eslamian 2014). Water is an important factor that showcases many of the effects of climate change on society, especially via the agriculture and energy sectors.

To increase the efficient use of available water, water management approaches are essential for both society and ecosystems (Leal Filho 2012). The blue water and green water concepts have introduced a new approach for water resources management, especially in arid and semi-arid regions where water scarcity is a serious issue (Zang et al. 2012). Blue water is the summation of water yield and deep aquifer recharge, green water flow is actual evapotranspiration, and green water storage is the soil water content (Falkenmark and Rockström 2006; Schuol et al. 2008a, b). These components are useful in identifying and managing the critical areas. Blue water is useful for socioeconomic development (Shiklomanov 2000; Döll

✉ Iman Fazeli Farsani
fazeligis@gmail.com

[1] Department of Soil Sciences, College of Agriculture, Shahrekord University, P.O. Box 115, Shahrekord, Iran

[2] Department of Water Engineering, Gorgan University of Agricultural Sciences and Natural Resources, Gorgan 49189-43464, Iran

[3] inter 3 GmbH - Institut für Ressourcenmanagement, Otto-Suhr-Allee 59, 10585 Berlin, Germany

[4] Department of Earth and Atmospheric Sciences, University of Alberta, Edmonton, AB T6G 2E3, Canada

Published online: 24 April 2018

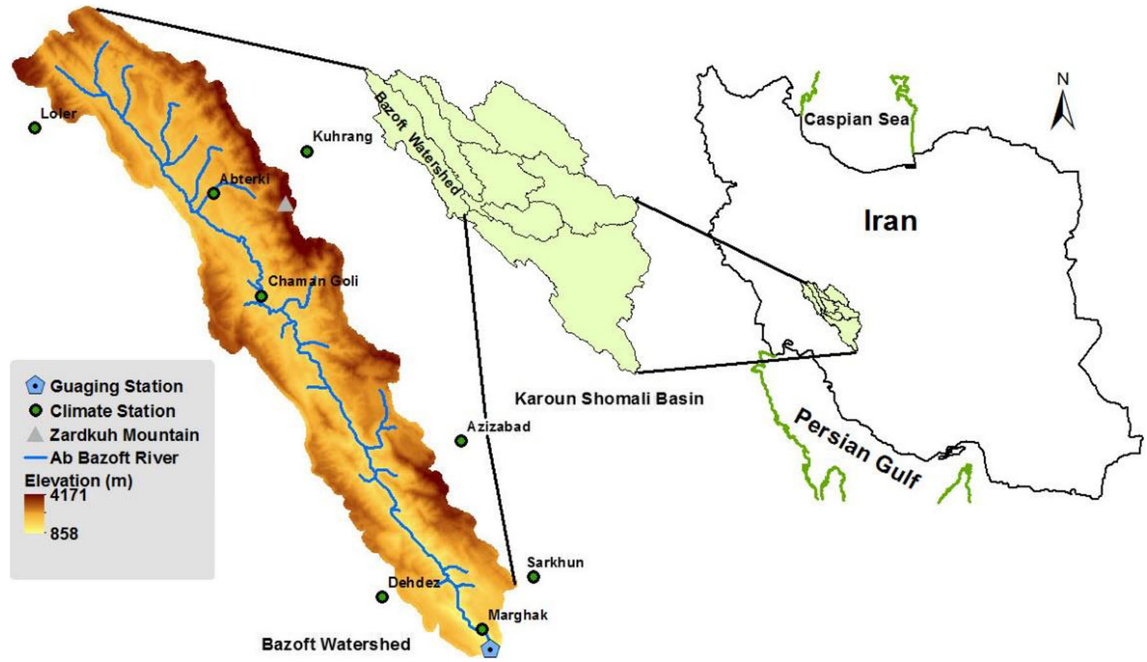

Fig. 1 Location of the study area and the selected meteorological and hydrological stations

2002; Zhang et al. 2014), green water is important for food supply and ecosystem health, and green water storage is the main water resource in rainfed agriculture (Rockström et al. 2009; Engdahl et al. 2012).

Investigating climate change impacts on water resources is important for long-term planning to achieve sustainable management of water resources (Zhang et al. 2014). Modeling tools can be useful for researchers and policy

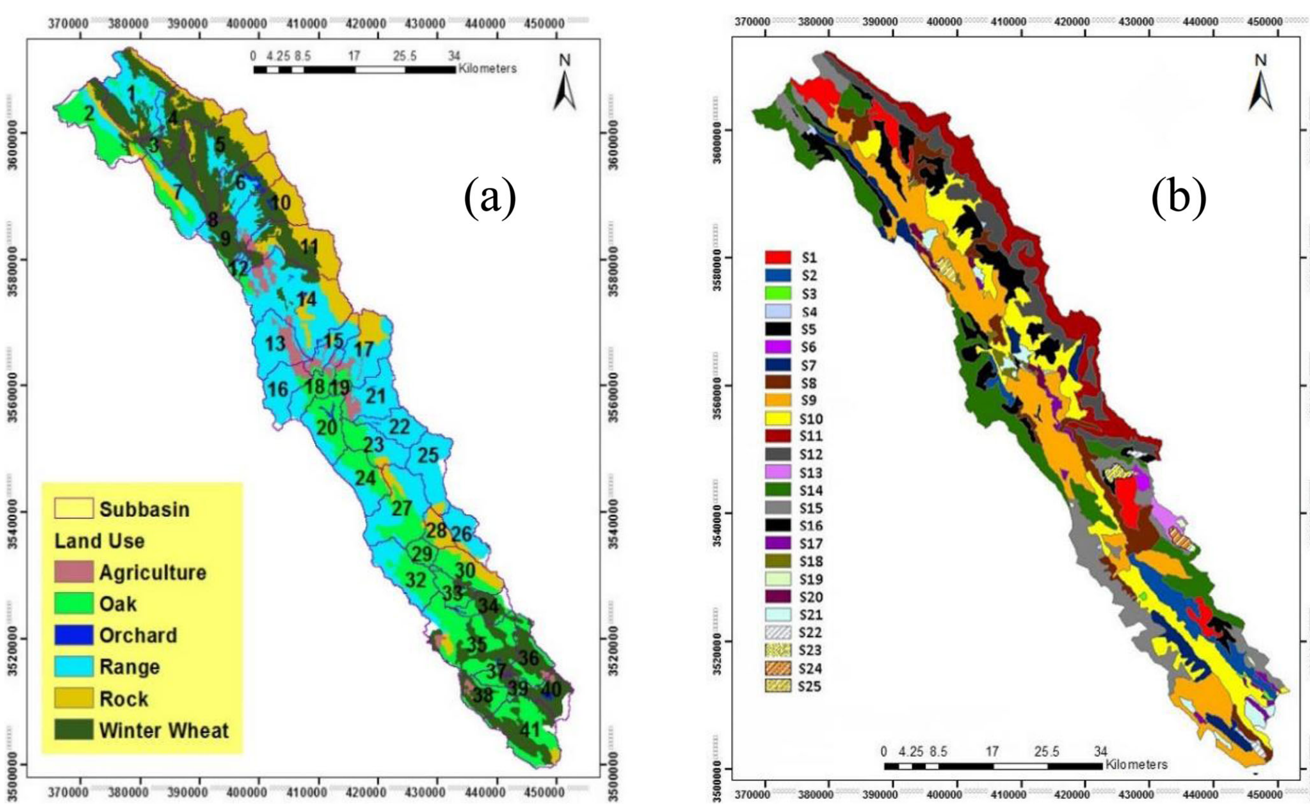

Fig. 2 Maps included in the SWAT model of the Bazoft watershed: (**a**) land use and (**b**) soil (S1-S25 are SWAT soil code/name in the SWAT databases)

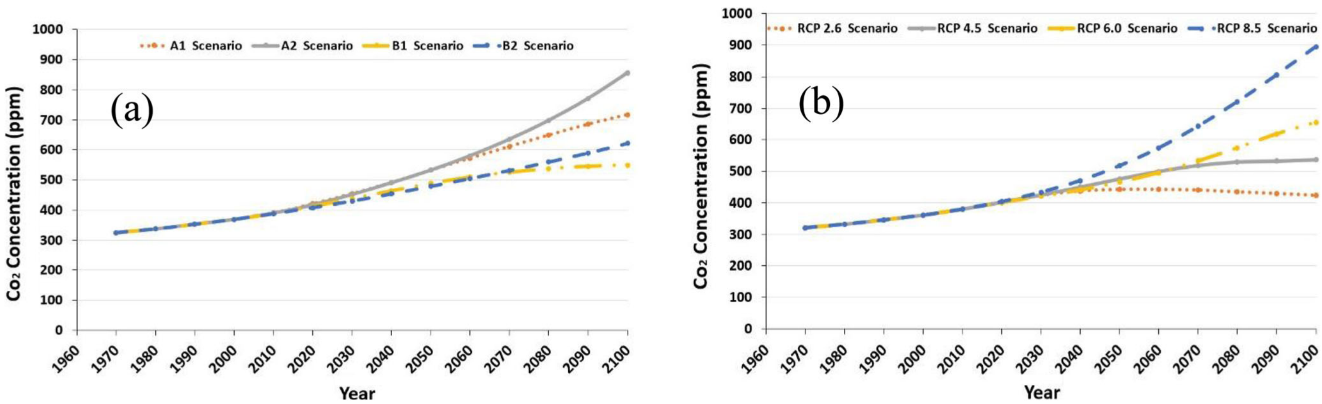

Fig. 3 CO_2 concentrations during 1960–2100 of **a** AR4 and **b** AR5 under different scenarios

Fig. 4 The results of simulated monthly discharges during calibration and validation periods

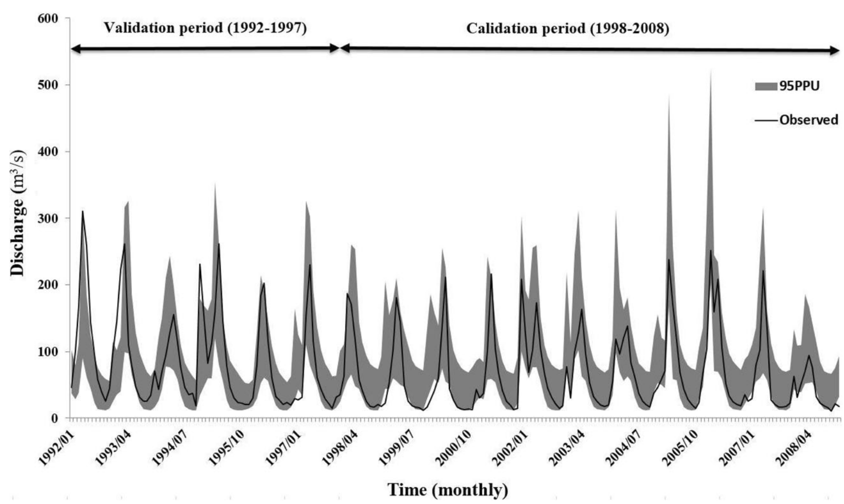

makers as tools for decision-making (Zang et al. 2012). Fakhri et al. (2014) investigated 72 hydrological models and reported that the soil and water assessment tool (SWAT) model is one of the most efficient in watershed modeling. Many studies (e.g., Abbaspour et al. 2009; Faramarzi et al. 2009; Ashraf Vaghefi et al. 2013; Faramarzi et al. 2013; Li et al. 2014, 2015, Shrestha et al. 2015) have shown that the SWAT model is a useful tool for investigating climate change effects on water resources. Faramarzi et al. (2013) investigated freshwater availability under climate change scenarios in Africa using the SWAT model. Although their models provide insightful information at the regional scale, the spatial resolution of input data was too large to assess water resources at a watershed scale and the monthly changes of blue water and green water could not be considered at the local scale. Many other studies have analyzed spatiotemporal changes of blue and green water resources at the basin level, but climate change effects have not been investigated (e.g., Zang et al. 2012; Rouholahnejad et al. 2014; Zhang et al. 2014; Zuo et al. 2015). Furthermore, blue and green water resources have been investigated using scenarios derived from the IPCC's Fourth Assessment Report (AR4) (e.g., Lee and Bae 2015) but rarely from the IPCC's Fifth Assessment Report (AR5).

The IPCC Special Report on Emissions Scenarios (SRES) defined four emission scenarios: A1, A2, B1,

Table 1 Summary statistics of simulated monthly discharges during calibration and validation periods

Discharge station		Evaluation criteria			
		R^2	NS	*p-factor*	*r-factor*
Marghak	Calibration	0.80	0.80	0.89	1.02
	Validation	0.57	0.59	0.76	1.03

R^2 coefficient of determination, *NS* Nash-Sutcliff coefficient, *p-factor* percentage of data being bracketed by 95PPU and B2. Each scenario represents various changing factors (e.g., population growth, economic growth, advances in technology, environmental characteristics, etc.), while AR5 adopts a different approach and the four new scenarios called representative concentration pathways (RCPs) (2.6, 4.5, 6.5, and 8.5), which are not directly comparable with the SRES scenarios (Clarke et al. 2014; IPCC 2007). The IPCC AR5 scenario is based primarily on results from the Coupled Model Intercomparison Project Phase 5 (CMIP5), promoted by the World Climate Research Program (WCRP), and it relies on results from CMIP3 modeling (Knutti and Sedláček 2013). The model range depicted in AR5 is slightly narrower than that in AR4, but uncertainty is still an issue that must be managed by users of new information (Urich et al. 2013). Knutti and Sedláček (2013) compared projections from CMIP3 and

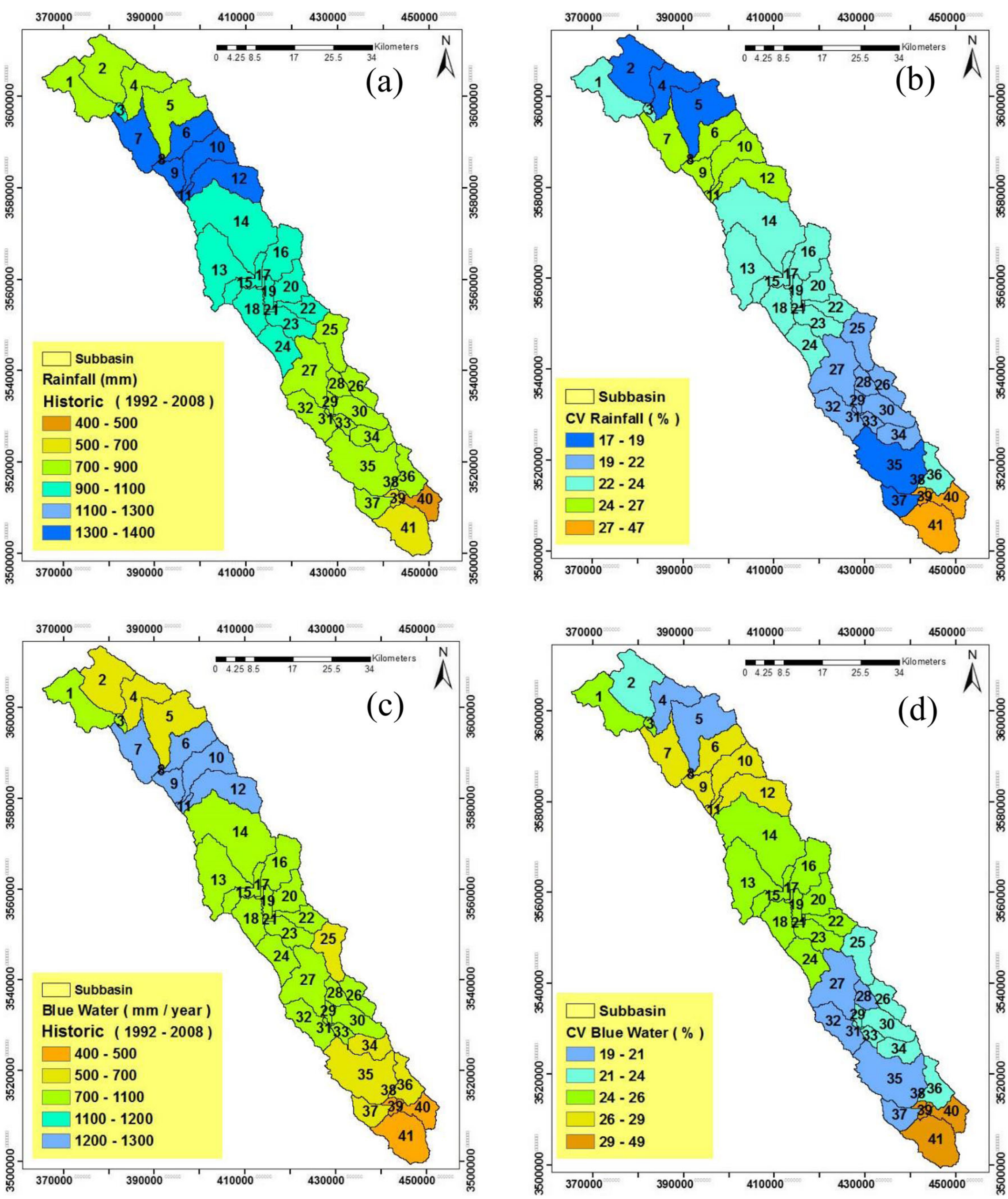

Fig. 5 The spatial pattern of the average (**a**, **c**) and variation coefficients (**b**, **d**) of rainfall and blue water resources calculated based on the average annual M95PPU values during 1992–2008

CMIP5 to look for convergence. They showed that mean patterns of rainfall and temperature change are similar between CMIP3 and CMIP5 at the global scale. Two remaining questions are how to interpret the lack of model convergence at the local scale, and what the uncertainties of water resource components are in CMIP3 and CMIP5 at the local scale, a topic that will be covered in this manuscript.

In this study, we investigated changes in various water resources in the context of climate change, and their uncertainties at the local scale. Our main objectives were (1) to calibrate and validate the SWAT model to analyze spatiotemporal water resource components at the sub-basin level with monthly time-steps and (2) to interpret uncertainties in various water resource components in the context of climate change based on IPCC AR4 and AR5 at the local scale.

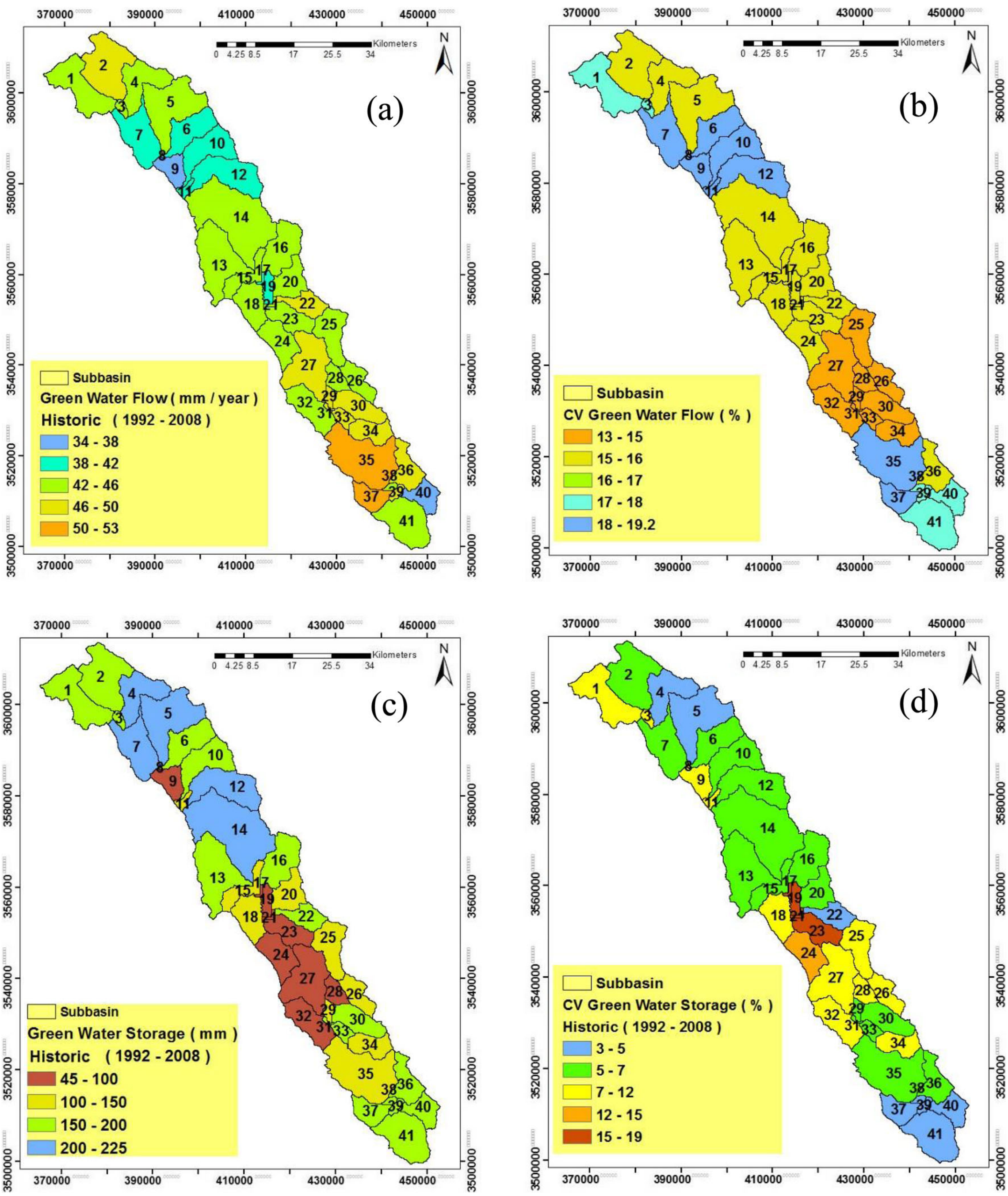

Fig. 6 The spatial pattern of mean (**a**, **c**), and variation coefficients (**b**, **d**) of green water flow and green water storage calculated based on the average annual M95PPU values during 1992–2008

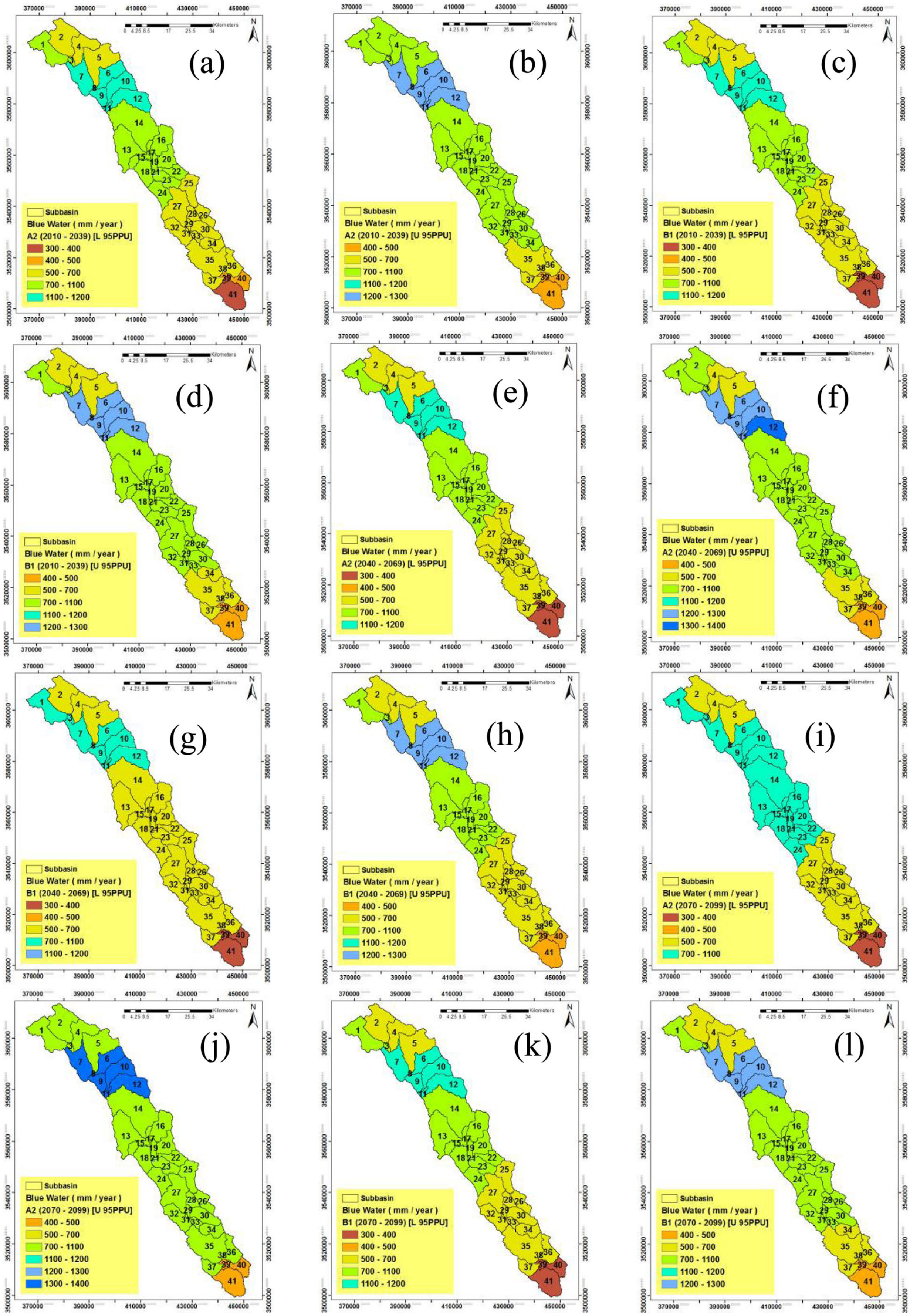
(a)
Subbasin
Blue Water (mm / year)
A2 (2010 - 2039) [L 95PPU]
300 - 400
400 - 500
500 - 700
700 - 1100
1100 - 1200
(b)
Subbasin
Blue Water (mm / year)
A2 (2010 - 2039) [U 95PPU]
400 - 500
500 - 700
700 - 1100
1100 - 1200
1200 - 1300
(c)
Subbasin
Blue Water (mm / year)
B1 (2010 - 2039) [L 95PPU]
300 - 400
400 - 500
500 - 700
700 - 1100
1100 - 1200
(d)
Subbasin
Blue Water (mm / year)
B1 (2010 - 2039) [U 95PPU]
400 - 500
500 - 700
700 - 1100
1100 - 1200
1200 - 1300
(e)
Subbasin
Blue Water (mm / year)
A2 (2040 - 2069) [L 95PPU]
300 - 400
400 - 500
500 - 700
700 - 1100
1100 - 1200
(f)
Subbasin
Blue Water (mm / year)
A2 (2040 - 2069) [U 95PPU]
400 - 500
500 - 700
700 - 1100
1100 - 1200
1200 - 1300
1300 - 1400
(g)
Subbasin
Blue Water (mm / year)
B1 (2040 - 2069) [L 95PPU]
300 - 400
400 - 500
500 - 700
700 - 1100
1100 - 1200
(h)
Subbasin
Blue Water (mm / year)
B1 (2040 - 2069) [U 95PPU]
400 - 500
500 - 700
700 - 1100
1100 - 1200
1200 - 1300
(i)
Subbasin
Blue Water (mm / year)
A2 (2070 - 2099) [L 95PPU]
300 - 400
400 - 500
500 - 700
700 - 1100
(j)
Subbasin
Blue Water (mm / year)
A2 (2070 - 2099) [U 95PPU]
400 - 500
500 - 700
700 - 1100
1100 - 1200
1200 - 1300
1300 - 1400
(k)
Subbasin
Blue Water (mm / year)
B1 (2070 - 2099) [L 95PPU]
300 - 400
400 - 500
500 - 700
700 - 1100
1100 - 1200
(l)
Subbasin
Blue Water (mm / year)
B1 (2070 - 2099) [U 95PPU]
400 - 500
500 - 700
700 - 1100
1100 - 1200
1200 - 1300

◀ **Fig. 7** Spatial pattern of blue water means predicted using bootstrap technique at the 2.5% (L95PPU) and 97.5% (U95PPU) uncertainty levels during 2010-2099, with possible changes in the AR4 scenarios from five GCMs (CGCM2, CISRO, ECHAM, HadCM3 and PCM)

2 Material and methods

2.1 Study area

The study area is the Bazoft watershed located between 31° 37′–32° 39′ N and 49° 34′–50° 32′ E in Iran (Fig. 1). The elevation ranges from 880 m in the south to 4200 m on Zardkuh Mountain in the northeast (Fig. 1). The long-term average rainfall and temperature are 800 mm and 10 °C, respectively. *Quercus brantii* and *Astragalus* spp. are the most abundant species of forest tree and pastures, respectively. Rainfall varies within the watershed, wherein average rainfall in the north is 1400 mm, and average rainfall in the south is < 500 mm due to the high-relief topography.

2.2 Hydrological modeling

2.2.1 SWAT model

The SWAT model is a semi-distributed, semi-physically based, basin-scale, temporally continuous model (Neitsch et al. 2009; Fakhri et al. 2014). It has been applied widely at different scales including the continental scale (e.g., Abbaspour et al. 2015; Faramarzi et al. 2013), national scale (e.g., Faramarzi et al. 2009), and regional scale (e.g., Zhang et al. 2014; Rodrigues et al. 2014).

2.2.2 Model data input and setup

The basic input data for the SWAT model comprised a digital elevation model (DEM), land use, soil type, and meteorological data. We first used a 30 m × 30 m grid size DEM, plus land use and soil layers. Climatic data including daily precipitation and temperature were obtained from the synoptic, climatological, and rain gauge stations located in the study area for a period of 20 years (1989–2008). Figures 1 and 2 show the maps (such as DEM, soil, and stream networks) included in the SWAT model. The entire simulation period was from 1989 to 2008, wherein the first 3 years (from 1989 to 1991) were considered as warm up period.

2.2.3 Sensitivity analysis, calibration, and validation

We used one-at-a-time method for the sensitivity analysis. Calibration, validation, and uncertainty analyses were done through the SUFI-2 program (Abbaspour 2012). Two thirds of the monthly discharge data (from 1998 to 2008) were used for calibration and the remaining one third (from 1992 to 1997) were used for validation. P-factor and R-factor indices were used to quantify the calibration performance.

2.2.4 Mass balance in SWAT model

The general water balance equation in the SWAT model is shown by Eq. (1) where each of the components can be involved in blue water and green water flow or storage (van Griensven et al. 2012; Rodrigues et al. 2014).

$$\begin{aligned}\text{Rainfall} &= \text{Evapotranspiration} + \text{Water Yeild} \\ &\quad + \Delta(\text{Soil Storage}) + \Delta\ \text{Groundwater Storage} \\ &\quad + \text{Losses} \end{aligned} \tag{1}$$

Blue water is the sum of the water yield (SWAT output WYLD) and deep aquifer recharge (SWAT output DA_RCHG) during the time step. Green water flow is represented by the actual evapotranspiration (SWAT output ET), and green water storage is the amount of water in the soil profile at the end of a time period (SWAT output SW), as suggested by Schuol et al. (2008b).

2.3 Global climate models and emission scenarios

General circulation models (GCMs) are used to determine future climate conditions, and various research institutes around the world have developed their own models. We obtained GCM data from the IPCC Data Distribution Center (http://www.ipcc-data.org/index.html) for each scenario. We used the GCM/SRES data from AR4 and the GCM/RCP data from AR5. In this study, we analyzed the hydrological models for the 2010–2039, 2040–2069, and 2070–2099 future periods. The set consisted of 18 model-scenarios including of CGCM2, CISRO, ECHAM, HadCM3, and PCM models from AR4, and GFDL, HADGEMES, IPSL, MROC, and NOEResm models from AR5. For the AR4 models, we used A2 and B1 scenarios, while for the AR5 models, we used RCP 2.6 and RCP 8.5 trajectories.

2.3.1 Change factor method

GCM climate projections have large uncertainties, and it is unreasonable to use the GCM simulation data directly at local scales (Murphy et al. 2004; Jung et al. 2013). Statistical downscaling techniques use the coarse resolution of GCMs at regional scales to

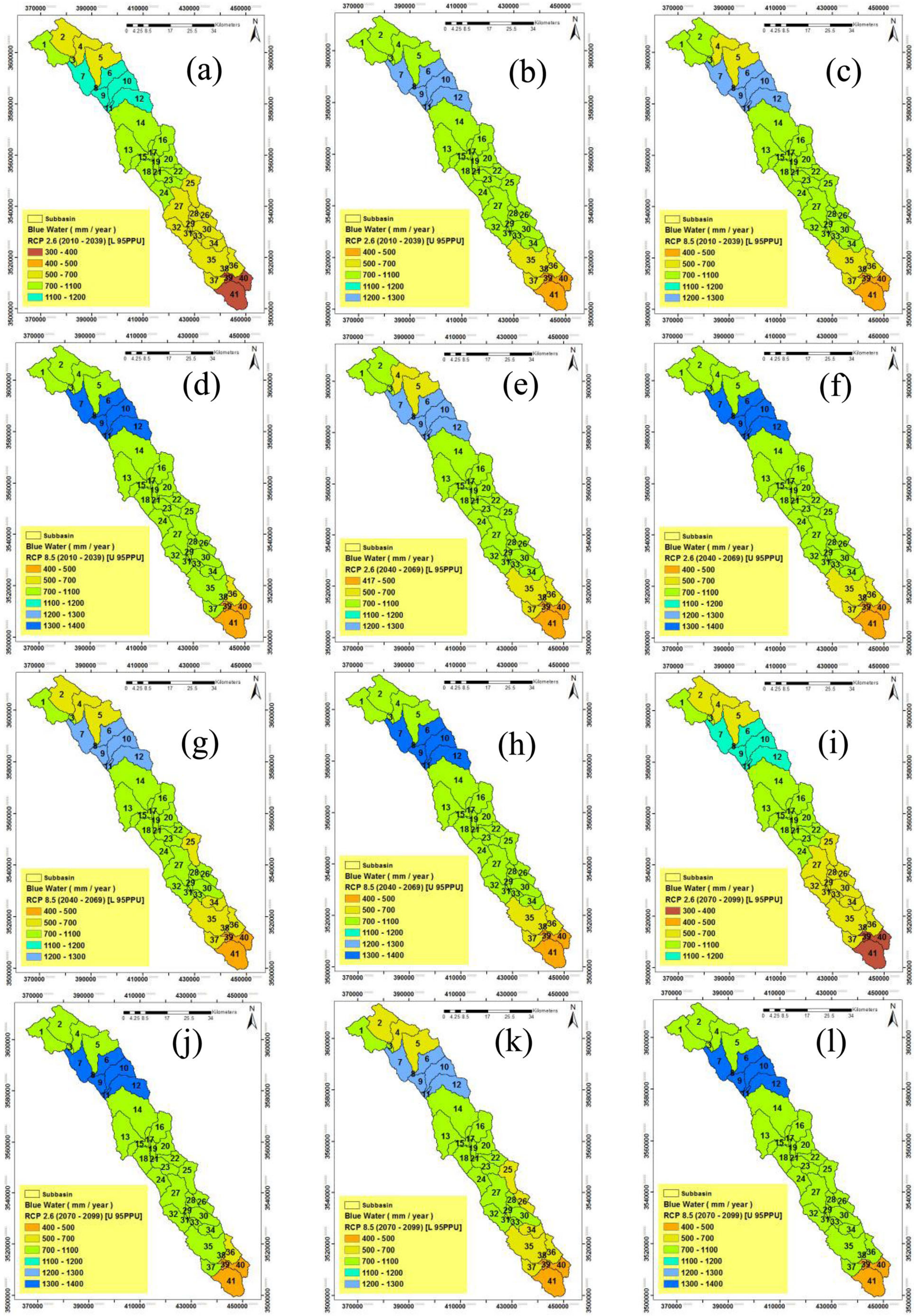
(a)
Subbasin
Blue Water (mm / year)
RCP 2.6 (2010 - 2039) [L 95PPU]
300 - 400
400 - 500
500 - 700
700 - 1100
1100 - 1200
(b)
Subbasin
Blue Water (mm / year)
RCP 2.6 (2010 - 2039) [U 95PPU]
400 - 500
500 - 700
700 - 1100
1100 - 1200
1200 - 1300
(c)
Subbasin
Blue Water (mm / year)
RCP 8.5 (2010 - 2039) [L 95PPU]
400 - 500
500 - 700
700 - 1100
1100 - 1200
1200 - 1300
(d)
Subbasin
Blue Water (mm / year)
RCP 8.5 (2010 - 2039) [U 95PPU]
400 - 500
500 - 700
700 - 1100
1100 - 1200
1200 - 1300
1300 - 1400
(e)
Subbasin
Blue Water (mm / year)
RCP 2.6 (2040 - 2069) [L 95PPU]
417 - 500
500 - 700
700 - 1100
1100 - 1200
1200 - 1300
(f)
Subbasin
Blue Water (mm / year)
RCP 2.6 (2040 - 2069) [U 95PPU]
400 - 500
500 - 700
700 - 1100
1100 - 1200
1200 - 1300
1300 - 1400
(g)
Subbasin
Blue Water (mm / year)
RCP 8.5 (2040 - 2069) [L 95PPU]
400 - 500
500 - 700
700 - 1100
1100 - 1200
1200 - 1300
(h)
Subbasin
Blue Water (mm / year)
RCP 8.5 (2040 - 2069) [U 95PPU]
400 - 500
500 - 700
700 - 1100
1100 - 1200
1200 - 1300
1300 - 1400
(i)
Subbasin
Blue Water (mm / year)
RCP 2.6 (2070 - 2099) [L 95PPU]
300 - 400
400 - 500
500 - 700
700 - 1100
1100 - 1200
(j)
Subbasin
Blue Water (mm / year)
RCP 2.6 (2070 - 2099) [U 95PPU]
400 - 500
500 - 700
700 - 1100
1100 - 1200
1200 - 1300
1300 - 1400
(k)
Subbasin
Blue Water (mm / year)
RCP 8.5 (2070 - 2099) [L 95PPU]
400 - 500
500 - 700
700 - 1100
1100 - 1200
1200 - 1300
(l)
Subbasin
Blue Water (mm / year)
RCP 8.5 (2070 - 2099) [U 95PPU]
400 - 500
500 - 700
700 - 1100
1100 - 1200
1200 - 1300
1300 - 1400

◀ **Fig. 8** Spatial pattern of blue water means predicted using bootstrap technique at the 2.5% (L95PPU) and 97.5% (U95PPU) uncertainty levels during 2010-2099, with possible changes in the AR5 scenarios from five GCMs (GFDL, HADGEMES, IPSL, MROC and NOEResm)

establish relationships among the GCM output, climate variables, and the local climate (Fowler et al. 2007). The change factor is a method for downscaling the course spatial and temporal resolution and can be implemented for different timescales such as daily, monthly, or longer periods (Zahmatkesh et al. 2014). Many studies use the change factor for downscaling climatic variables (e.g., Diaz-Nieto and Wilby 2005; Tabor and Willams 2010; Abdolhosseini and Farzaneh 2014; Zahmatkesh et al. 2014).

We used the change factor method to downscale precipitation and temperature. In this method, to obtain future regional condition, climate change scenarios are added to observed values via Eqs. (2) and (3):

$$P = P_{base} \times \Delta P \tag{2}$$

$$T = T_{base} + \Delta T \tag{3}$$

where P and T are time series of precipitation and temperature in the future period, P_{base} and T_{base} express observed time series of monthly precipitation and temperature in the base period, and ΔP and ΔT relate to a downscaled climate change scenario, respectively.

CO_2 concentration is an important factor for climate change impact assessment because an integrated depiction of climate change depends on the emission of CO_2 and the corresponding climate response (Jha et al. 2006). Figure 3 shows the CO_2 concentration in different scenarios in AR4 and AR5. We calculated CO_2 concentrations for three future periods (2010–2039, 2040–2069, 2070–2099) for use in the SWAT model.

2.4 Bootstrap technique

Using the results of the model for different scenarios of GCM/SRES/RCP, we used a bootstrap technique to analyze the uncertainties of the outputs (Efron 1979). The bootstrap method is a simple procedure used to estimate the required values in a specific statistical pattern for simulating parameter distributions (Fakhri et al. 2013). The resulting uncertainty is quantified by using the 95PPU, calculated at the 2.5 and 97.5% levels of the cumulative distribution of an output variable obtained through bootstrapping.

3 Results and discussion

3.1 Sensitivity analysis, calibration, and uncertainty analysis

CN2, temperature, precipitation, and surface runoff lag time coefficient (SURLAG) were the most sensitive parameters. The results of simulated discharges at the monthly time scale during the calibration and validation periods are presented in Fig. 4. We found that the discharge simulations during the historical period (1992–2008) were accurate. Obtained evaluation criteria of the r-factor, p-factor, R^2, and Nash–Sutcliff coefficients were 1.02, 0.89, 0.80, and 0.80 for the calibration period and 1.03, 0.76, 0.57, and 0.59 for the validation period, respectively (Table 1).

3.2 Quantification of water resource availability

We calculated the 95PPU at the monthly time scale using the simulation results at the 2.5 and 97.5% uncertainty levels. We used the simulated results at the 50% uncertainty level (M95PPU) to calculate changes of variables relative to the corresponding historical simulations during 1992–2008. Since GCMs have various uncertainties associated with climate change impacts on hydrological processes, 18 different scenarios were used for impact assessment.

All scenarios extracted from the SWAT outputs of water resource components, using the bootstrap technique at the 2.5 and 97.5% uncertainty levels, were used to capture minimum and maximum uncertainties in the future.

3.2.1 Availability of blue and green water resources at the sub-basin scale during the historical period

Figure 5c shows the average values of blue water (mm/year) based on historical data during 1992–2008. In general, blue water increased in the northern part of the watershed. Most of blue water (1300–1400 mm) occurred in sub-basins 6 through 12. These are mostly covered by snow in fall and winter, and sub-basins with snow and melting water often have more blue water. The least blue water (400–500 mm) was observed in sub-basins 39 to 41. The spatial pattern of blue water was mainly influenced by the spatial pattern of rainfall (Fig. 5a, c). However, rainfall distribution depends on elevation, and sub-basins 6 to 12 are at the highest elevation, while sub-basins 39 to 41 are at the lowest. The total difference in elevation throughout the watershed is 3300 m, and rainfall varies between 400 and 1400 mm/year. Overall, both rainfall and blue water per sub-basin in the Bazoft watershed decreased from upstream to downstream (Fig. 5).

We mapped the long-term (1992–2008) averages of green water flow and storage for the watershed, along with their coefficients of variation (Fig. 6). In contrast to blue

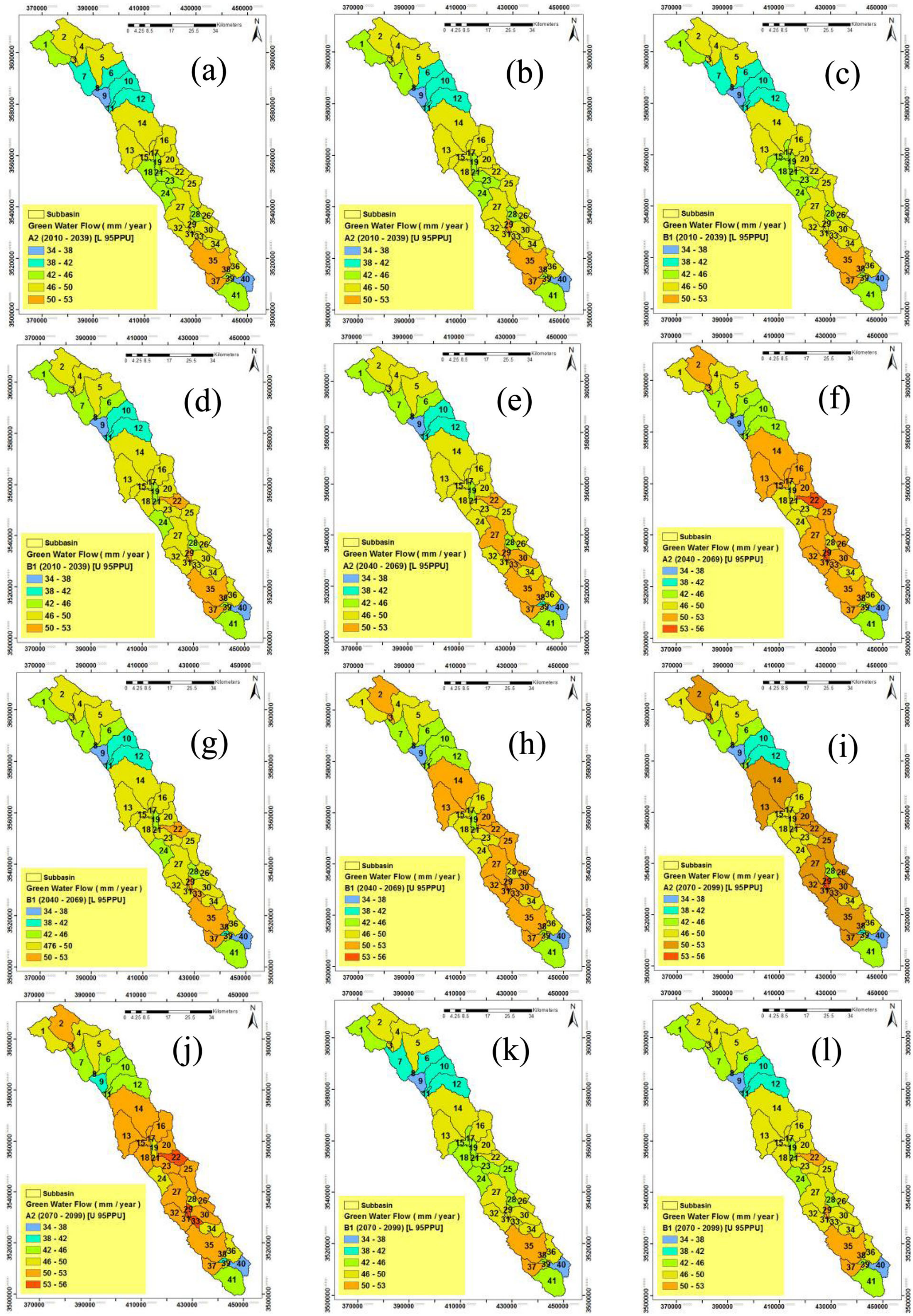
(a)
Subbasin
Green Water Flow (mm / year)
A2 (2010 - 2039) [L 95PPU]
34 - 38
38 - 42
42 - 46
46 - 50
50 - 53
(b)
Subbasin
Green Water Flow (mm / year)
A2 (2010 - 2039) [U 95PPU]
34 - 38
38 - 42
42 - 46
46 - 50
50 - 53
(c)
Subbasin
Green Water Flow (mm / year)
B1 (2010 - 2039) [L 95PPU]
34 - 38
38 - 42
42 - 46
46 - 50
50 - 53
(d)
Subbasin
Green Water Flow (mm / year)
B1 (2010 - 2039) [U 95PPU]
34 - 38
38 - 42
42 - 46
46 - 50
50 - 53
(e)
Subbasin
Green Water Flow (mm / year)
A2 (2040 - 2069) [L 95PPU]
34 - 38
38 - 42
42 - 46
46 - 50
50 - 53
(f)
Subbasin
Green Water Flow (mm / year)
A2 (2040 - 2069) [U 95PPU]
34 - 38
38 - 42
42 - 46
46 - 50
50 - 53
53 - 56
(g)
Subbasin
Green Water Flow (mm / year)
B1 (2040 - 2069) [L 95PPU]
34 - 38
38 - 42
42 - 46
476 - 50
50 - 53
(h)
Subbasin
Green Water Flow (mm / year)
B1 (2040 - 2069) [U 95PPU]
34 - 38
38 - 42
42 - 46
46 - 50
50 - 53
53 - 56
(i)
Subbasin
Green Water Flow (mm / year)
A2 (2070 - 2099) [L 95PPU]
34 - 38
38 - 42
42 - 46
46 - 50
50 - 53
53 - 56
(j)
Subbasin
Green Water Flow (mm / year)
A2 (2070 - 2099) [U 95PPU]
34 - 38
38 - 42
42 - 46
46 - 50
50 - 53
53 - 56
(k)
Subbasin
Green Water Flow (mm / year)
B1 (2070 - 2099) [L 95PPU]
34 - 38
38 - 42
42 - 46
46 - 50
50 - 53
(l)
Subbasin
Green Water Flow (mm / year)
B1 (2070 - 2099) [U 95PPU]
34 - 38
38 - 42
42 - 46
46 - 50
50 - 53

◀ **Fig. 9** Spatial pattern of green water flow means predicted using bootstrap technique at the 2.5% (L95PPU) and 97.5% (U95PPU) uncertainty levels during 2010-2099, with possible changes in the AR4 scenarios from five GCMs (CGCM2, CISRO, ECHAM, HadCM3 and PCM)

water, green water flow decreased from upstream to downstream in the watershed. Green water flow is mainly influenced by land cover in these areas. Forest and winter wheat are the main land cover types in the south, especially in sub-basins 34 to 41, while most northern and central sub-basins are dominated by rangeland and rock. Overall, green water flows are distributed more homogeneously among sub-basins than were blue water flows. Precipitation is high in upstream sub-basins, but evapotranspiration is relatively small, potentially due to low temperature. In downstream sub-basins, precipitation is low and temperature is higher, meaning that most precipitation evaporates directly into the atmosphere. Furthermore, field observations have shown that soil depth in most regions is less than 10 cm, especially in sub-basins 6 to 12; consequently, evaporation from soil and transpiration from vegetation of the sub area is too low.

While the green water storage was relatively high (Fig. 6c), the amount of blue water in the southern portion of the watershed was low (Fig. 5c), which may be related to the forest's capacity to hold soil moisture. In most of the northern sub-basins, and especially in sub-basins 6 to 12 where soil depth was low, the amount of green water storage was high. This is mainly due to the snow and melting water that cause higher green water storage in the low-depth soils. The central sub-basins had the lowest green water storage because of their low soil depths and predominantly rangeland cover types.

To determine the annual variation of water resource components from 1992 to 2008, we calculated the coefficient of variation (CV in %):

$$CV = \frac{\sigma}{\mu} \times 100 \tag{4}$$

where σ is the standard deviation and μ is the mean value of annual water resource components for each sub-basin. A high CV indicates a region vulnerable to extreme weather conditions such as drought (Abbaspour et al. 2015). Figures 5b, d and 6b, d illustrate the CV of historical water resource components for each sub-basin. In general, the CV was lowest for green water storage and largest for blue water. For blue water, blue regions were more reliable in terms of their water resources (Fig. 5d). Areas with greater soil moisture and smaller CV indicate a higher potential for the development of rainfed farming (Fig. 6d).

3.2.2 Impact of climate change on water resource components

The maps of all components are provided for the future periods of 2010–2039, 2040–2069, and 2070–2099 to showcase relationships between climate change and hydrological components.

Figures 7 and 8 show the mean values of blue water during 2010–2099 with possible changes in the AR4 and AR5 scenarios at the 2.5% (L95PPU) and 97.5% (U95PPU) uncertainty levels. Trends for blue water showed considerable spatial variation among sub-basins (Fig. 7). In general, blue water decreased during the future simulation periods. Although the U95PPU of the blue water increased in the B1 (2010–2039, Fig. 7d) and A2 (2070–2099, Fig. 7j) scenarios, in most periods, it showed a decreasing trend compared to the historical period (Figs. 5c and 7). The L95PPU of blue water reached its minimum in A2 (2070–2099, Fig. 7j). Overall, the A2 scenario (2070–2099, Fig. 7i, j) illustrates the upper and lower limits of blue water in the future. Changes in blue water flow in the AR4 scenarios (Fig. 7) were consistent with those in the AR5 scenarios (Fig. 8) over most periods and in most parts of the area, except the northernmost and southernmost sub-basins. RCP 2.6 (U95PPU, 2070–2099, Fig. 8j) and RCP 8.5 (U95PPU, 2010–2039 and 2070–2099, Fig. 8d, l) illustrate the maximum value of blue water. Minimum conditions are illustrated in RCP 2.6 (L95PPU, 2010–2039 and 2070–2099, Fig. 8a, i). Generally, the amount of blue water flow in most AR5 scenarios was higher than under the AR4 scenarios (Figs. 7 and 8).

Figures 9 and 10 illustrate the average values of green water flow predicted based on the future period of 2010–2099. Future changes in green water flow show more heterogeneous conditions in different scenarios, periods, and sub-basins than do those of blue water and green water storage. In general, green water flow increased in the downstream and midstream basins, but we found low spatial variation among the northern sub-basins compared to the historical period (Figs. 6a, 9, and 10). The U95PPU in A2 (2070–2099) illustrates the maximum value of green water flow (Fig. 9j). Overall, Fig. 10 shows that the value of green water flow in the AR5 scenarios is greater than that in the AR4 scenarios (Figs. 9 and 10).

At the all-basin scale, past trends in green water storage will persist into the future (see Figs. 6c and 11). Since there were no differences among future periods, only two maps, at the 2.5 and 97.5% uncertainty levels, are presented in Fig. 11.

3.2.3 Blue and green water resource availability at the monthly time scale

Figure 12 shows the SWAT 95PPU ranges of water resource component monthly averages for 1992–2008 under the 18

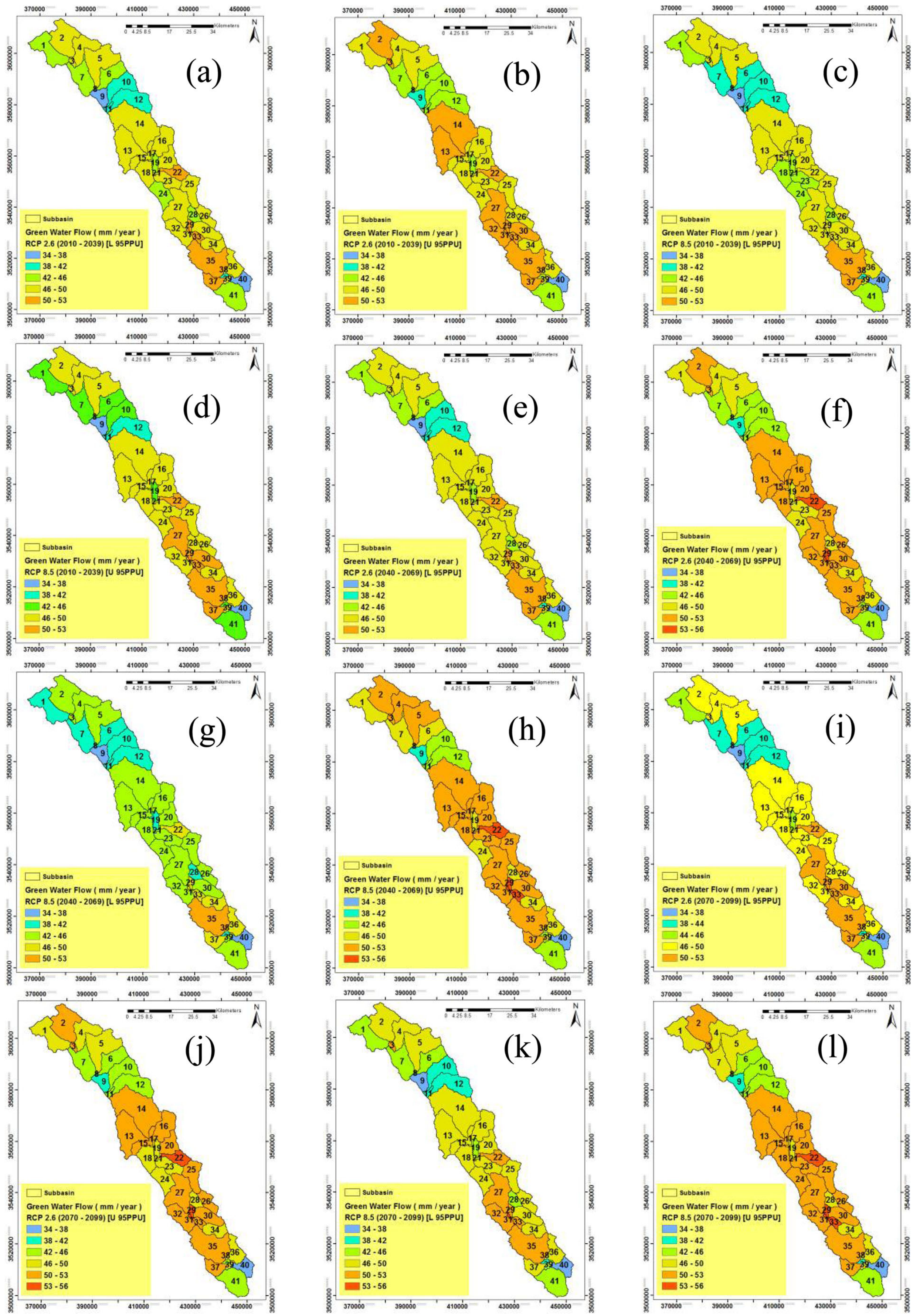
(a)
Subbasin
Green Water Flow (mm / year)
RCP 2.6 (2010 - 2039) [L 95PPU]
34 - 38
38 - 42
42 - 46
46 - 50
50 - 53
(b)
Subbasin
Green Water Flow (mm / year)
RCP 2.6 (2010 - 2039) [U 95PPU]
34 - 38
38 - 42
42 - 46
46 - 50
50 - 53
(c)
Subbasin
Green Water Flow (mm / year)
RCP 8.5 (2010 - 2039) [L 95PPU]
34 - 38
38 - 42
42 - 46
46 - 50
50 - 53
(d)
Subbasin
Green Water Flow (mm / year)
RCP 8.5 (2010 - 2039) [U 95PPU]
34 - 38
38 - 42
42 - 46
46 - 50
50 - 53
(e)
Subbasin
Green Water Flow (mm / year)
RCP 2.6 (2040 - 2069) [L 95PPU]
34 - 38
38 - 42
42 - 46
46 - 50
50 - 53
(f)
Subbasin
Green Water Flow (mm / year)
RCP 2.6 (2040 - 2069) [U 95PPU]
34 - 38
38 - 42
42 - 46
46 - 50
50 - 53
53 - 56
(g)
Subbasin
Green Water Flow (mm / year)
RCP 8.5 (2040 - 2069) [L 95PPU]
34 - 38
38 - 42
42 - 46
46 - 50
50 - 53
(h)
Subbasin
Green Water Flow (mm / year)
RCP 8.5 (2040 - 2069) [U 95PPU]
34 - 38
38 - 42
42 - 46
46 - 50
50 - 53
53 - 56
(i)
Subbasin
Green Water Flow (mm / year)
RCP 2.6 (2070 - 2099) [L 95PPU]
34 - 38
38 - 44
44 - 46
46 - 50
50 - 53
(j)
Subbasin
Green Water Flow (mm / year)
RCP 2.6 (2070 - 2099) [U 95PPU]
34 - 38
38 - 42
42 - 46
46 - 50
50 - 53
53 - 56
(k)
Subbasin
Green Water Flow (mm / year)
RCP 8.5 (2070 - 2099) [L 95PPU]
34 - 38
38 - 42
42 - 46
46 - 50
50 - 53
53 - 56
(l)
Subbasin
Green Water Flow (mm / year)
RCP 8.5 (2070 - 2099) [U 95PPU]
34 - 38
38 - 42
42 - 46
46 - 50
50 - 53
53 - 56

◀ **Fig. 10** Spatial pattern of green water flow means predicted using bootstrap technique at the 2.5% (L95PPU) and 97.5% (U95PPU) uncertainty levels during 2010–2099, with possible changes in the AR5 scenarios from five GCMs (GFDL, HADGEMES, IPSL, MROC and NOEResm)

scenarios. Many of these scenarios were located in our prediction uncertainties (see Fig. 12).

Uncertainties were larger for blue water and smaller for other components (Fig. 12b). This may be caused by a limited soil water supply as well as by soil evapotranspiration and the soil evaporation compensation factor (ESCO) parameter for green water flow and green water storage, respectively; most parameters used in the calibration procedure are involved in calculating blue water values. The large uncertainty could be caused by snow parameters not specially being defined in SWAT's classification, and runoff supply from melting snow and on frozen ground not being simulated in the SCS method. Similar issues have been reported in literature (Fontaine et al. 2002; Rostamian et al. 2008; Akhavana et al. 2010).

In Fig. 12b, the uncertainty is high from March to June because the watershed is dominated by spring snow melt. The region freezes sometime between Jan 1 and March 15 and staying frozen until the spring thaw, which can take place from March 15 to June.

In Fig. 12c, the uncertainty is low in fall and early winter because the biomass is minimal, while in spring and summer, the uncertainty is increased due to irrigation management in agricultural areas. Overall, in most months, the average uncertainty in future prediction was smaller than the lower bound of the historical prediction uncertainty (Fig. 12c).

Different climate change scenarios showed a narrow range in green water storage (Fig. 12d). The monthly average green water storage showed that in spring and summer, there is sufficient soil water; thus, the watershed has higher potential for the development of rainfed agriculture (Fig. 12d). Faramarzi et al. (2009) and Abbaspour et al. (2015) reported similar results for their study areas in Iran and Europe, respectively.

4 Conclusions

In this study, we successfully applied a sub-basin-scale hydrologic model at the monthly time scale to quantify water resource components and climate change impact assessments for the Bazoft watershed, Iran. The calibration and validation results were acceptable for river discharge. The impact assessment was done both spatially (sub-basin scale) and temporally (monthly time scale). Our results showed that hydrological

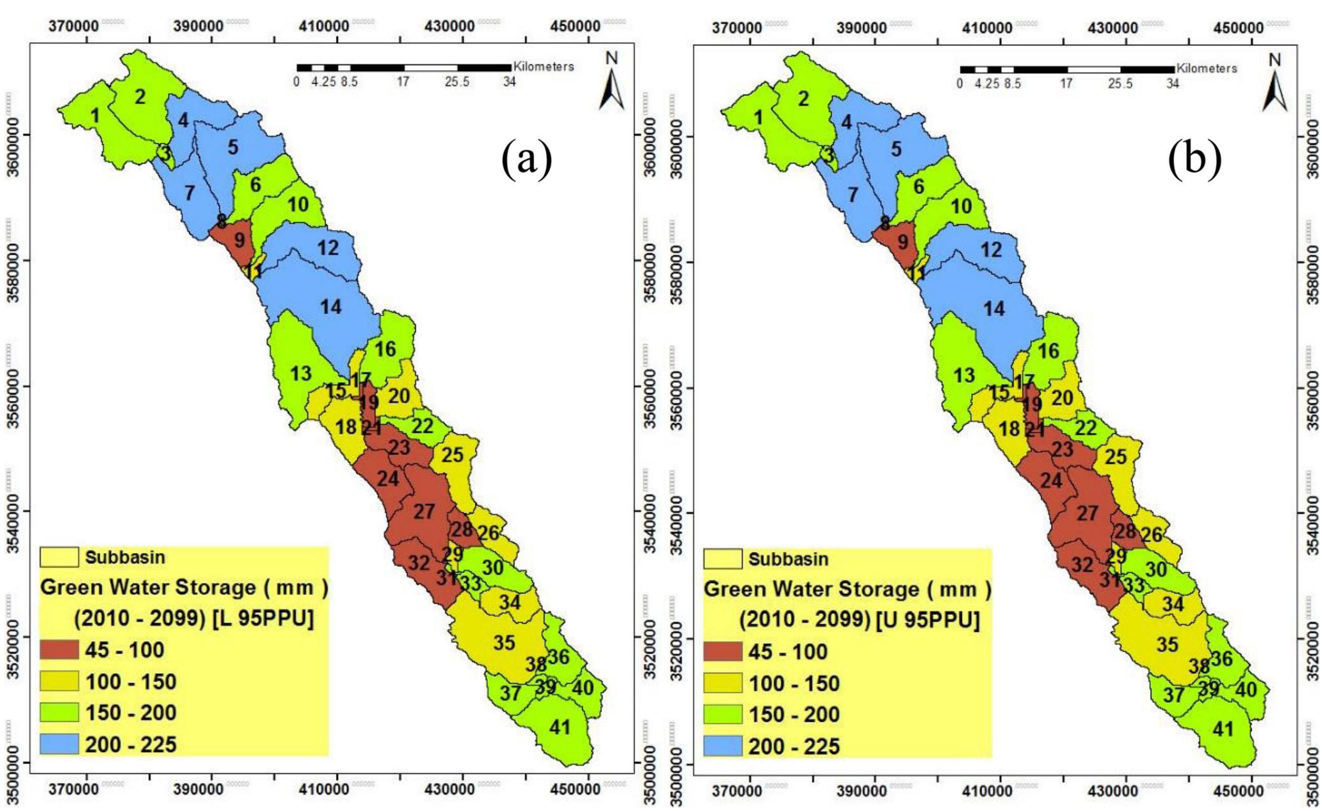

Fig. 11 Spatial pattern of green water flow means predicted using bootstrap technique at the 2.5% (L95PPU) and 97.5% (U95PPU) uncertainty levels during 2010–2099, with possible changes in the AR4 and AR5 scenarios from ten GCMs

Fig. 12 Average (1992–2008) monthly 95PPU ranges of **a** precipitation, **b** blue water, **c** green water flow, and **d** green water storage for the Bazoft watershed under 18 scenario impact assessments

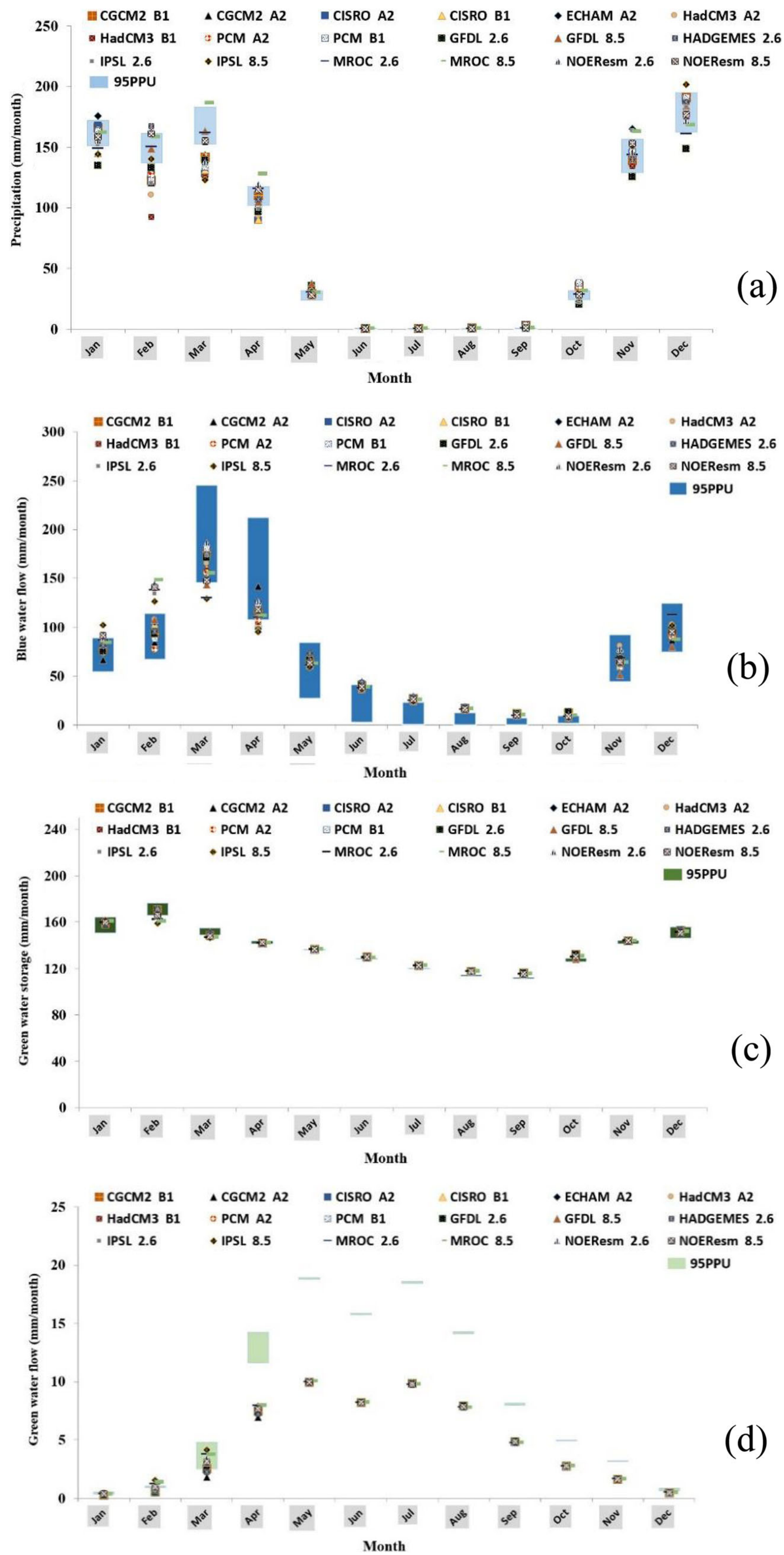

variables can differ among locations within a basin. The U95PPU and L95PPU in blue and green water flows varied widely across watershed.

Differences among the AR4 and AR5 scenarios might be due to the sources of uncertainty and their assumptions. At the watershed scale, blue water will continue decreasing in the future. We found that green water flow increased in the downstream and midstream sub-basins, but that there was low spatial variation among northern sub-basins compared to the historical period. We also found that green water storage will continue its historical trend in the future.

The uncertainties that we calculated for the historical period were negligible in green water flow and green water storage but were larger for green water flow because the supply of water to the soil and for evapotranspiration is limited by the soil's capacity and the ESCO parameter. However, most of parameters in the calibration procedure for blue water calculations, as well as for snow melt in March, April, May, and June, were available. Furthermore, different climate change predictions were within a narrow range in all months for green water storage. To increase accuracy and decrease uncertainties, we recommend considering climate change and land use changes simultaneously.

In our study, the spatial patterns of water resource components and their uncertainties in the context of climate change were notably different under the AR4 and AR5 scenarios at the local scale, while Knutti and Sedláček (2013) showed that climatic factors, including precipitation and temperature, were similar at the global scale. The differences between these climate change models are related to uncertainties and their underlying assumptions. All of these uncertainties are low when aggregated globally, especially for climate variables, whereas the effects of climate change are local and could differ among water resource variables. There is much spatial heterogeneity and larger uncertainty at the local scale. This study can be applied to other regions facing similar challenges to help assess the likely effects of climate change on water resource components and may help decision makers a global scale.

Acknowledgements The authors would like to thank the anonymous reviewers and the Editor in Chief for their valuable comments and suggestions. We also acknowledge the World Climate Research Program's (WCRP's) Working Group on Coupled Modeling (WGCM), which is responsible for CMIP, and the climate modeling groups (listed in Sect. 2.3 of this paper) for producing and making available their model output.

References

Abbaspour KC (2012) SWAT-CUP 2012: SWAT calibration and uncertainty programs—a user manual. Eawag: Swiss Fed. Inst. of Aquat. Sci. and Technol., Duebendorf, Switzerland, pp 103. Available at http://www.neprashtechnology.ca/downloads. Accessed 3 Dec 2016

Abbaspour KC, Faramarzi M, Ghasemi SS, Yang H (2009) Assessing the impact of climate change on water resources in Iran. Water Resour Res 45:W10434. https://doi.org/10.1029/2008WR007615

Abbaspour KC, Rouholahnejad E, Ashraf Vaghefi S, Srinivasan R, Yang H, Kløve B (2015) A continental-scale hydrology and water quality model for Europe: calibration and uncertainty of a high-resolution large-scale SWAT model. J Hydrol 524:733–752. https://doi.org/10.1016/j.jhydrol.2015.03.027

Abdolhosseini M, Farzaneh MR (2014) Investigation of internal uncertainty sources of change factor method in downscaling of climatic parameters of future period. Intl J Agric Crop Sci 7(12):941–949

Akhavana S, Abedi-Koupaia J, Mousavi SF, Afyuni M, Eslamian SS, Abbaspour KC (2010) Application of SWAT model to investigate nitrate leaching in Hamadan–Bahar watershed, Iran. Agric Ecosyst Environ 139:675–688. https://doi.org/10.1016/j.agee.2010.10.015

Ashraf Vaghefi S, Mousavi SJ, Abbaspour KC, Srinivasan R, Yang H (2013) Analyses of the impact of climate change on water resources components, drought and wheat yield in semiarid regions: Karkheh River Basin in Iran. Hydrol Process 28:2018–2032. https://doi.org/10.1002/hyp.9747

Clarke L, Jiang K, Akimoto K, Babiker M, Blanford G, Fisher-Vanden K, Hourcade JC, Krey V, Kriegler E, Löschel A, McCollum D, Paltsev S, Rose S, Shukla PR, Tavoni M, van der Zwaan BCC, van Vuuren DP (2014) Assessing transformation pathways. In Edenhofer O, Pichs-Madruga R, Sokona Y, Farahani E, Kadner S, Seyboth K, Adler A, Baum I, Brunner S, Eickemeier P, Kriemann B, Savolainen J, Schlömer S, von Stechow C, Zwickel T, Minx JC (eds) Climate change 2014: Mitigation of climate change. Contribution of Working Group III to the Fifth Assessment Report of the Intergovernmental Panel on Climate Change., Cambridge University Press, Cambridge, United Kingdom and New York, NY, USA

Diaz-Nieto J, Wilby RL (2005) A comparison of statistical downscaling and climate change factor methods: impacts on low flows in the river Thames, United Kingdom. Clim Chang 2:245–268. https://doi.org/10.1007/s10584-005-1157-6

Döll P (2002) Impact of climate change and variability on irrigation requirements: a global perspective. Clim Chang 54(3):269–293. https://doi.org/10.1023/A:1016124032231

Efron B (1979) Bootstrap methods: another look at the jackknife. Ann Stat 7:1–26

Engdahl NB, Ginn TR, Fogg GE (2012) Using groundwater age distributions to estimate the effective parameters of Fickian and non-Fickian models of solute transport. Adv Water Resour 54:11–21. https://doi.org/10.1016/j.advwatres.2012.12.008

Eslamian S (2014) Handbook of engineering hydrology: environmental hydrology and water management. CRC Press, Boca Raton

Fakhri M, Farzaneh MR, Eslamian SS, Khordadi MJ (2013) Confidence interval assessment to estimate dry and wet spells under climate change in Shahrekord station, Iran. J Hydrol Eng 18(7):911–918. https://doi.org/10.1061/(ASCE)HE.1943-5584.0000688

Fakhri M, Dokouhaki H, Eslamian SS, Fazeli Farsani I, Farzaneh MR (2014) Flow and sediment transport modeling in rivers. In: Eslamian SS (ed) Handbook of engineering hydrology, Ch. 13, Vol. 2: modeling, climate change, and variability. Taylor and Francis: CRC Press, Boca Raton, pp 233–267

Falkenmark M, Rockström J (2006) The new blue and green water paradigm: breaking new ground for water resources planning and management. J Water Resour Plan Manag 132(3):129–132. https://doi.org/10.1061/(ASCE)0733-9496(2006)132:3(129)

Faramarzi M, Abbaspour KC, Schulin R, Yang H (2009) Modelling blue and green water resources availability in Iran. Hydrol Process 23:486–501. https://doi.org/10.1002/hyp.7160

Faramarzi M, Abbaspour KC, Ashraf Vaghefi S, Farzaneh MR, Zehnder AJB, Sirinivasan R, Yang H (2013) Modeling impacts of climate change on freshwater availability in Africa. J Hydrol 480:85–101. https://doi.org/10.1016/j.jhydrol.2012.12.016

Fontaine TA, Cruickshank TS, Arnold JG, Hotchkiss RH (2002) Development of a snowfall–snowmelt routine for mountainous terrain for the soil water assessment tool (SWAT). J Hydrol 262(1–4): 209–223. https://doi.org/10.1016/S0022-1694(02)00029-X

Fowler HJ, Blenkinsop S, Tebaldi C (2007) Linking climate change modeling to impact studies: recent advances in downscaling techniques of hydrological modeling. Int J Climatol 27:1547–1578. https://doi.org/10.1002/joc.1556

IPCC (2007) Contribution of Working Group I to the Fourth Assessment Report of the Intergovernmental Panel on Climate Change. Solomon S, Qin D, Manning M, Chen Z, Marquis M, Averyt KB, Tignor M, Miller HL (eds). Cambridge University Press, Cambridge, United Kingdom and New York, NY, USA

IPCC (2014) Impacts, adaptation and vulnerability. Part A: Global and sectoral aspects. Contribution of Working Group II to the Fifth Assessment Report of the Intergovernmental Panel on Climate Change. Field CB, Barros VR, Dokken DJ, Mach KJ, Mastrandrea MD, Bilir TE, Chatterjee M, Ebi KL, Estrada YO, Genova RC, Girma B, Kissel ES, Levy AN, MacCracken S, Mastrandrea PR, White LL (eds). Cambridge University Press, Cambridge, United Kingdom and New York, NY, USA

Jha M, Arnold JG, Gassman PW, Giorgi F, Gu RR (2006) Climate change sensitivity assessment on upper Mississippi river basin streamflows using SWAT. J Am Water Resour Assoc 42(4):997–1015. https://doi.org/10.1111/j.1752-1688.2006.tb04510.x

Jung IW, Bae DH, Lee BJ (2013) Possible change in Korean streamflow seasonality multi-model climate projections. Hydrol Process 27(7): 1033–1045. https://doi.org/10.1002/hyp.9215

Knutti R, Sedláček J (2013) Robustness and uncertainties in the new CMIP5 climate model projections. Nat Clim Chang 3:369–373. https://doi.org/10.1038/nclimate1716

Leal Filho W (2012) Climate change and the sustainable use of water resources. Springer, New York

Lee M-H, Bae D-Hyo (2015) Climate change impact assessment on green and blue water over Asian Monsoon Region. Water Resour Manage 29(7):2407–2427. https://doi.org/10.1007/s11269-015-0949-3

Li B, Su H, Chen F, Li H, Zhang R, Tian J, Chen S, Yang Y, Rong Y (2014) Separation of the impact of climate change and human activity on streamflow in the upper and middle reaches of the Taoer River, northeastern China. Theor Appl Climatol 118(1):271–283. https://doi.org/10.1007/s00704-013-1032-8

Li Z, Lü Z, Li J, Shi X (2015) Links between the spatial structure of weather generator and hydrological modeling. Theor Appl Climatol 128(1–9):103–111. https://doi.org/10.1007/s00704-015-1691-8

Murphy JM, Sexton DMH, Barnett DN, Jones GS, Webb MJ, Collins M, Stainforth DA (2004) Quantification of modelling uncertainties in a large ensemble of climate change simulations. Nature 430:768–772. https://doi.org/10.1038/nature02771

Neitsch SL, Arnold JG, Kiniry JR, Williams JR (2009) Soil and water assessment tool, theoretical documentation, Version 2009. Agr. Res. Service and Blackland Res. Cent, Temple

Rockström J, Falkenmark M, Karlberg L, Hoff H, Rost S, Gerten D (2009) Future water availability for global food production: the potential of green water for increasing resilience to global change. Water Resour Res 45:W00A12. https://doi.org/10.1029/2007WR006767

Rodrigues DBB, Gupta HV, Mendiondo EM (2014) A blue/green water-based accounting framework for assessment of water security. Water Resour Res 50:7187–7205. https://doi.org/10.1002/2013WR014274

Rostamian R, Jaleh A, Afyuni M, Mousavi SF, Heidarpour M, Jalalian A, Abbaspour KC (2008) Application of a SWAT model for estimating runoff and sediment in two mountainous basins in Central Iran. Hydrol Sci J 53(5):977–988. https://doi.org/10.1623/hysj.53.5.977

Rouholahnejad E, Abbaspour KC, Srinivasan R, Bacu V, Lehmann A (2014) Water resources of the Black Sea basin at high spatial and temporal resolution. Water Resour Res 50:5866–5885. https://doi.org/10.1002/2013WR014132

Schuol J, Abbaspour KC, Srinivasan R, Yang H (2008a) Estimation of freshwater availability in the west African sub-continent using the SWAT hydrologic model. J Hydrol 352(1–2):30–49. https://doi.org/10.1016/j.jhydrol.2007.12.025

Schuol J, Abbaspour KC, Srinivasan R, Yang H (2008b) Modelling blue and green water availability in Africa. Water Resour Res 44: W07406. https://doi.org/10.1029/2007WR006609

Shiklomanov IA (2000) Appraisal and assessment of world water resources. Water Int 25(1):11–32. https://doi.org/10.1080/02508060008686794

Shrestha S, Shrestha M, Babel MS (2015) Assessment of climate change impact on water diversion strategies of Melamchi water supply project in Nepal. Theor Appl Climatol 128:1–13. https://doi.org/10.1007/s00704-015-1713-6

Tabor K, Willams J (2010) Global downscaled climate projections for assessing the conservation impacts of climate change. Ecol Appl 20:554–565. https://doi.org/10.1890/09-0173.1

Urich PB, Kouwenhoven P, Li Y (2013) The IPCC fifth assessment report in context: implications for end users in the transition from AR4. A CLIMsystems Technical Report; 15 pp.

Van Griensven A, Ndomba P, Yalew S, Kilonzo F (2012) Critical review of SWAT applications in the upper Nile basin countries. Hydrol Earth Syst Sci 16(9):3371–3381. https://doi.org/10.5194/hess-16-3371-2012

Zahmatkesh Z, Karamouz M, Goharian E, Burian SJ, Tavakol-Davani H (2014) Climate change impacts on urban runoff in a New York City watershed. In World Environ Water Resour Congress 2014:938–951. https://doi.org/10.1061/9780784413548.096

Zang CF, Liu J, van der Velde M, Kraxner F (2012) Assessment of spatial and temporal patterns of green and blue water flows under natural conditions in inland river basins in Northwest China. Hydrol Earth Syst Sci 16:2859–2870. https://doi.org/10.5194/hess-16-2859-2012

Zhang W, Zha X, Li J, Liang W, Ma Y, Fan D, Li S (2014) Spatiotemporal change of blue water and green water resources in the Headwater of Yellow River Basin, China. Water Resour Manage 28(13):4715–4732. https://doi.org/10.1007/s11269-014-0769-x

Zuo D, Xu Z, Peng D, Jinxi S, Cheng L, Wei S, Abbaspour KC, Yang H (2015) Simulating spatiotemporal variability of blue and green water resources availability with uncertainty analysis. Hydrol Process 29: 1942–1955. https://doi.org/10.1002/hyp.10307